

**Tetraphenylethene -functionalized diketopyrrolopyrrole solid state
emissive molecules: enhanced emission in the solid state and as a
fluorescent probe for cyanide detection**

Lingyun Wang ^{a*}, Linhui Zhu^a, Lin Li ^{b*}, Derong Cao ^a

^a School of Chemistry and Chemical Engineering, State Key Laboratory of Luminescent Materials and Devices, South China University of Technology, Guangzhou, China, 510641

^b School of Food Science and Engineering, South China University of Technology, Guangzhou, China, 510641

*Corresponding author: Tel. +86 20 87110245; fax: +86 20 87110245. E-mail:

lingyun@scut.edu.cn; felinli@scut.edu.cn

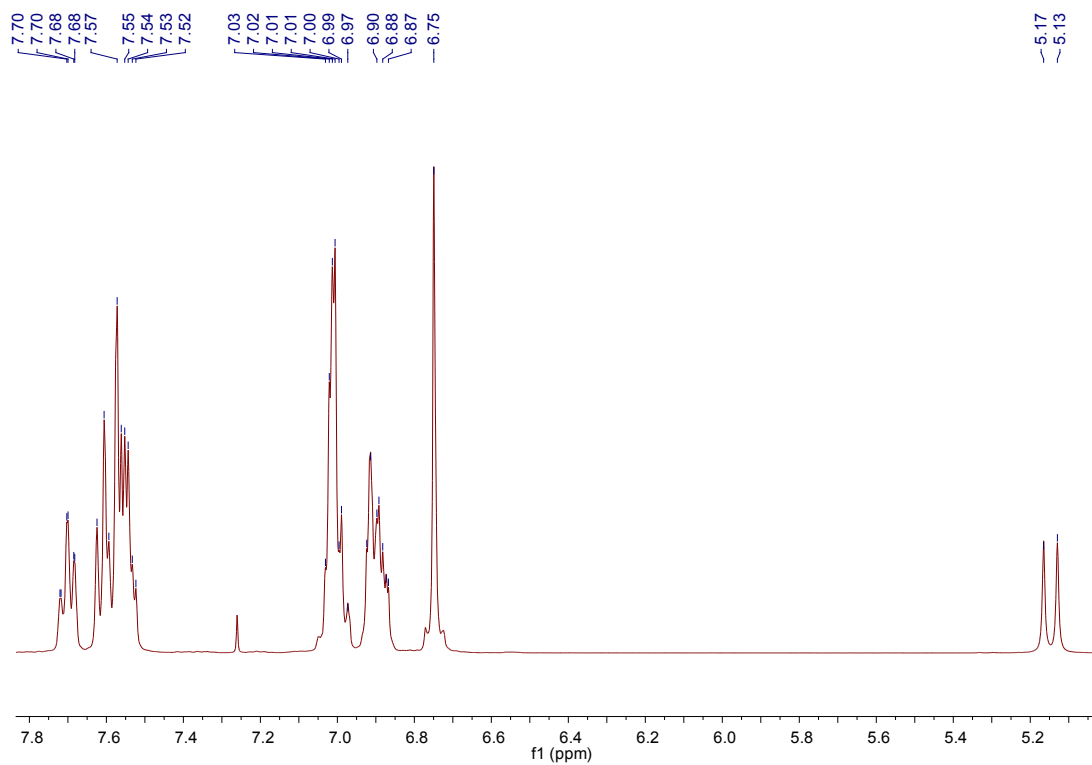


Fig.S1 ^1H NMR spectrum of compound **7** in CDCl_3 .

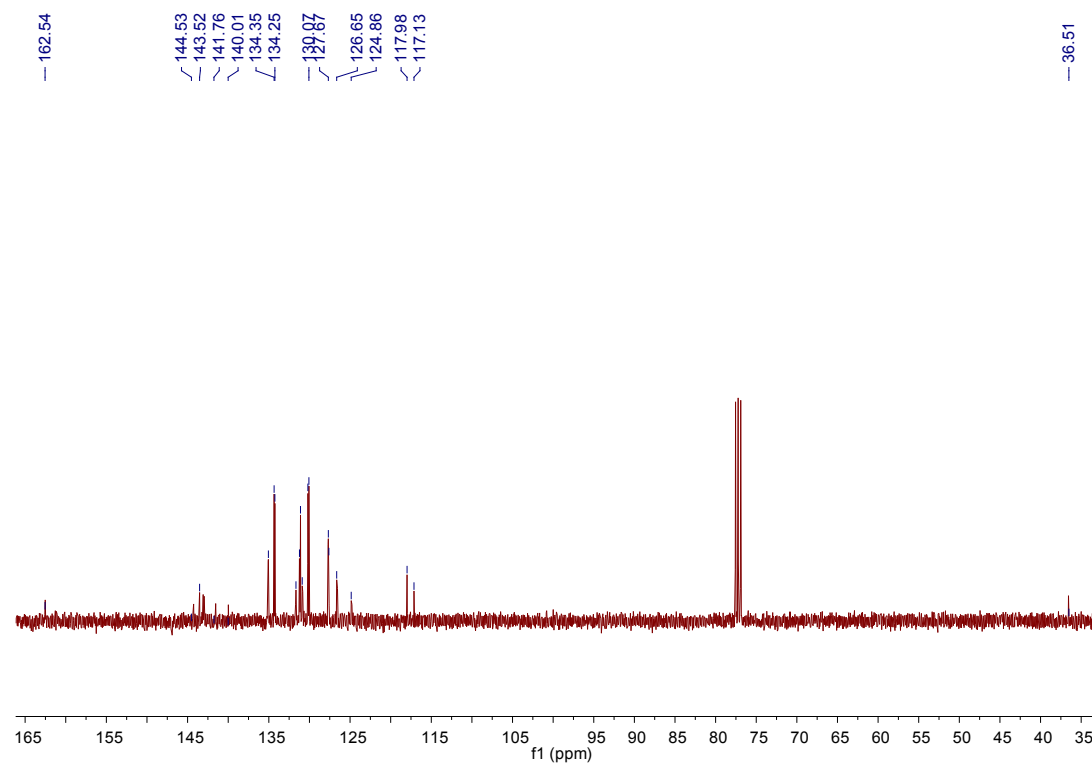


Fig.S2 ^{13}C NMR spectrum of compound **7** in CDCl_3 .

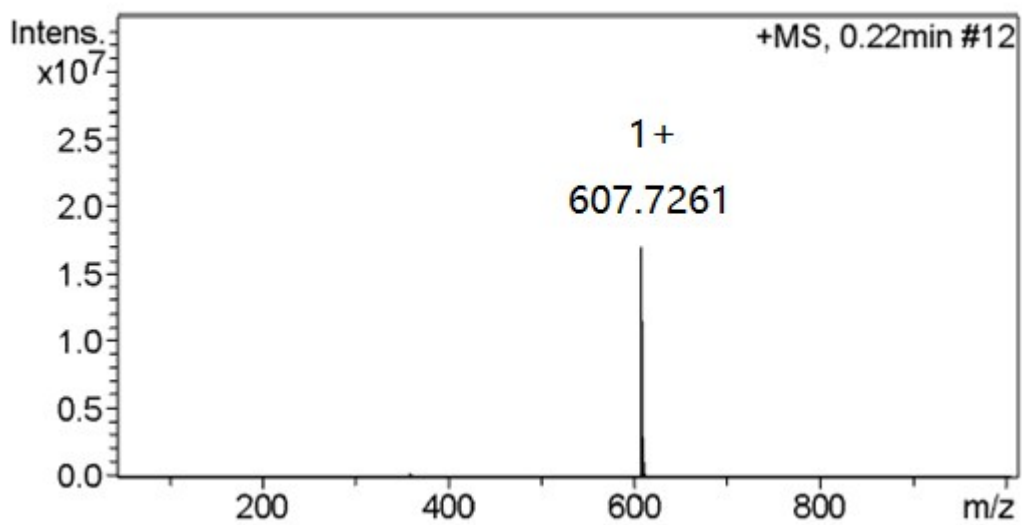


Fig.S3 HRMS spectrum of compound 7.

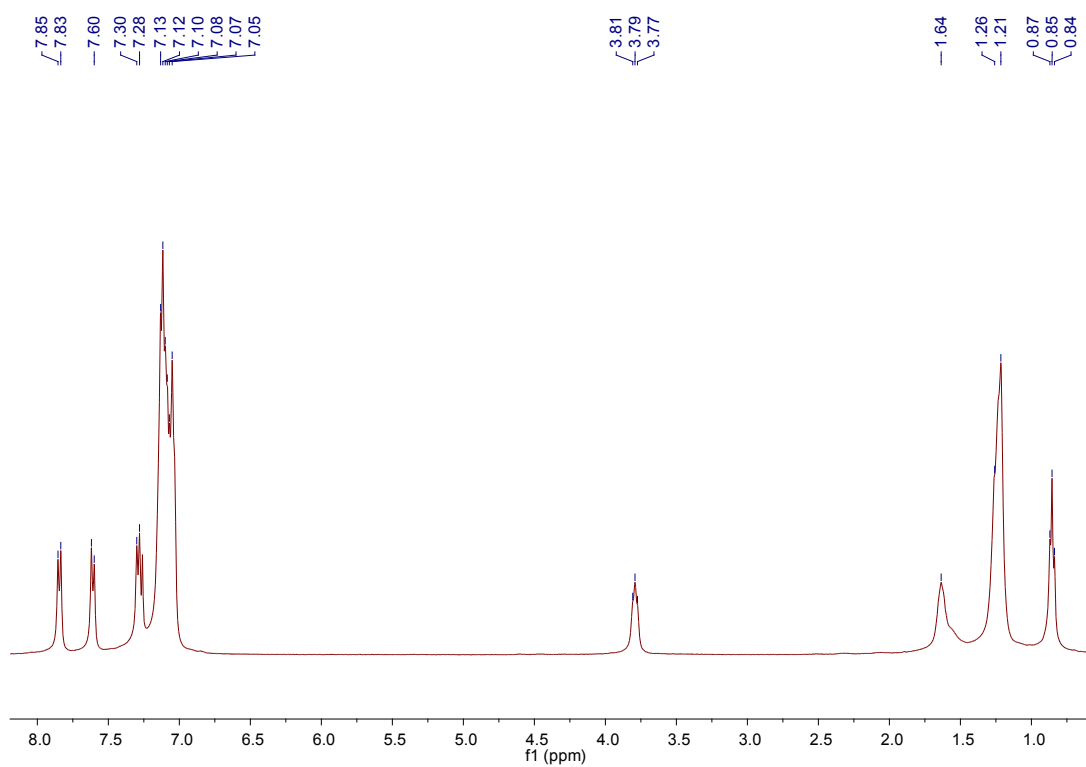


Fig.S4 ¹H NMR spectrum of **DPP1** in CDCl₃.

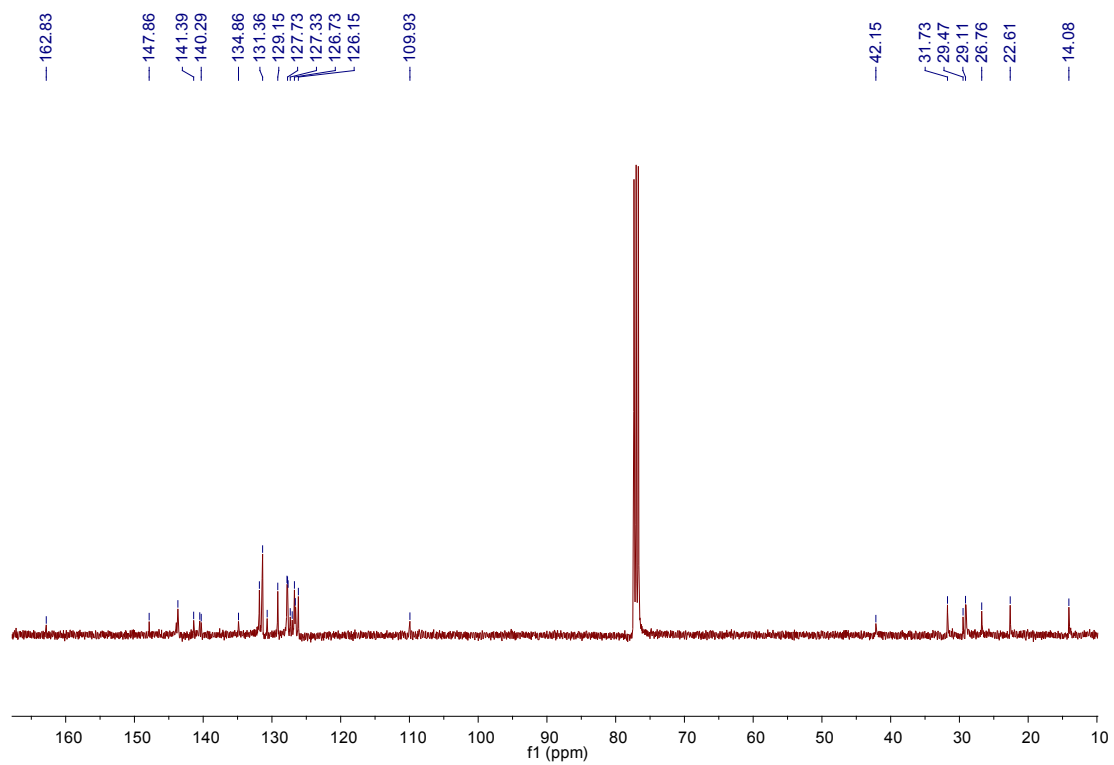


Fig.S5 ^{13}C NMR spectrum of **DPP1** in CDCl_3 .

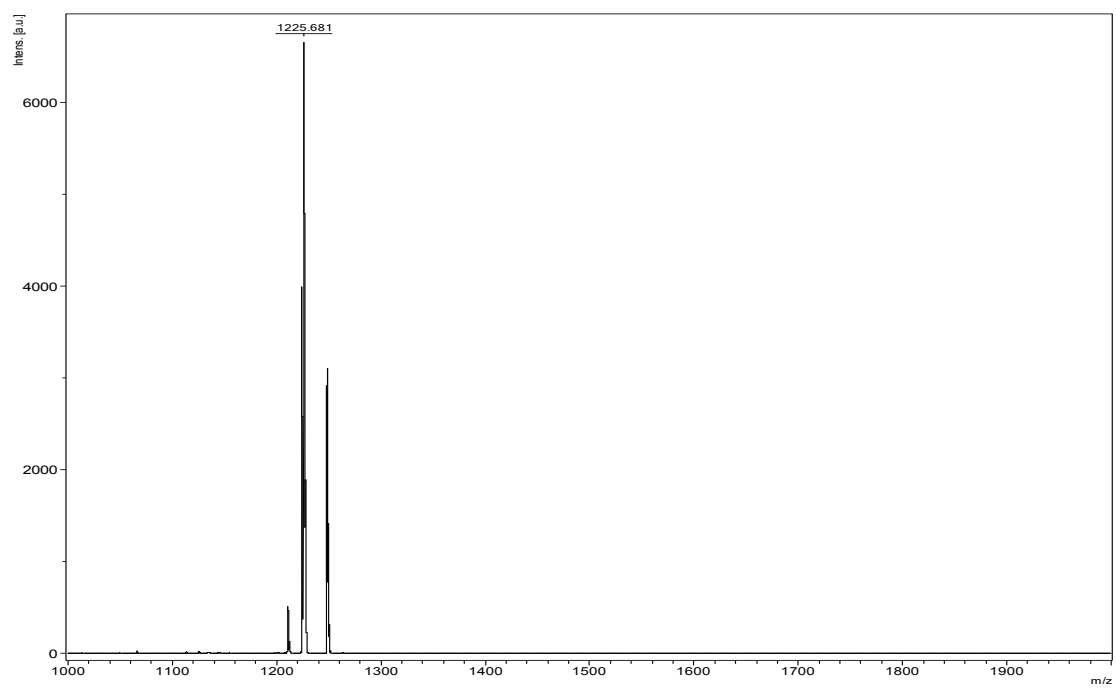


Fig.S6 HRMS spectrum of **DPP1**.

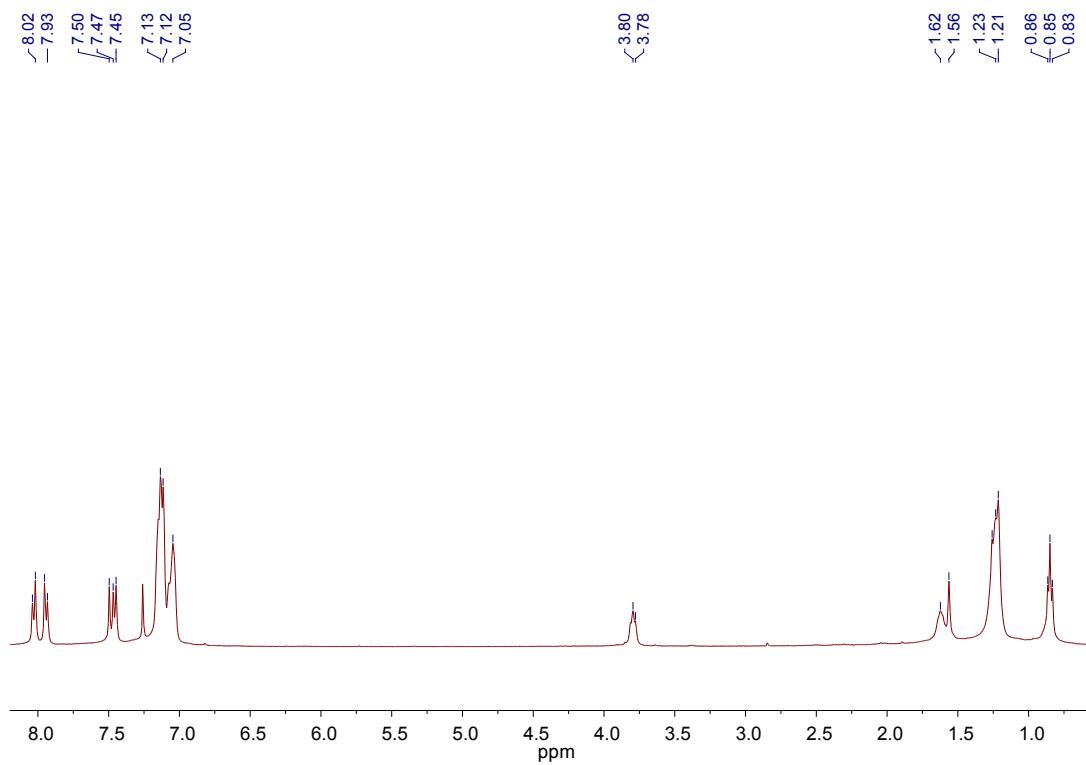


Fig.S7 ^1H NMR spectrum of **DPP2** in CDCl_3 .

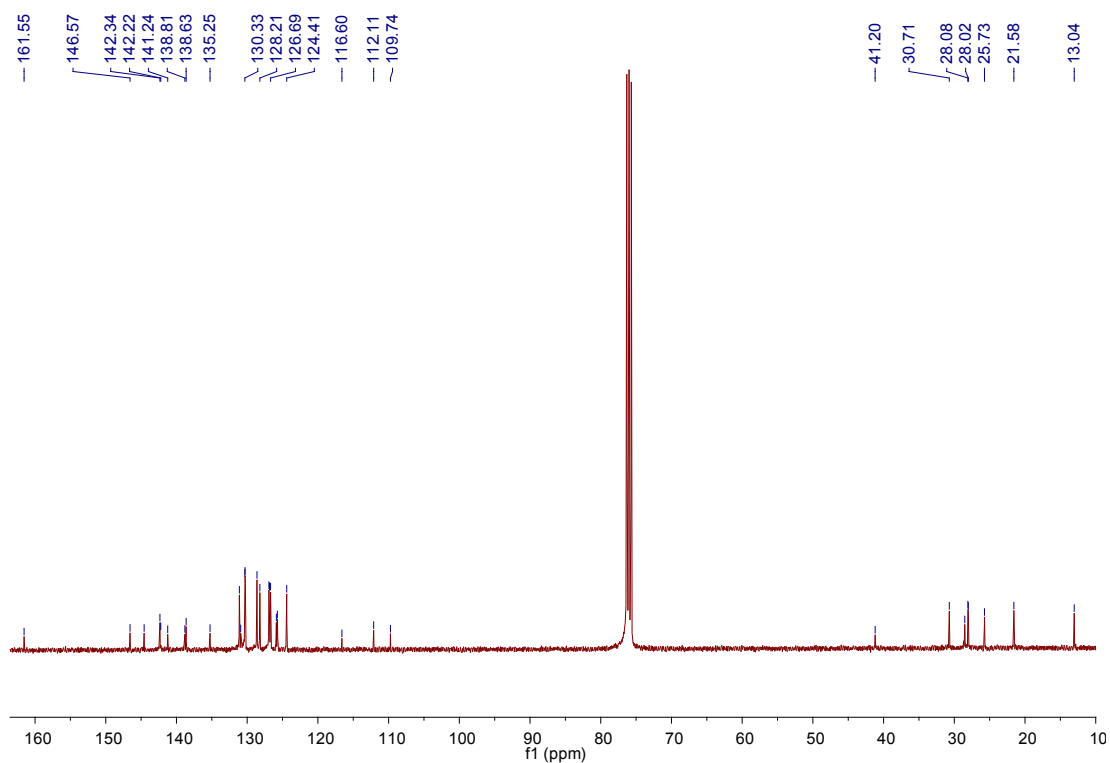


Fig.S8 ^{13}C NMR spectrum of **DPP2** in CDCl_3 .

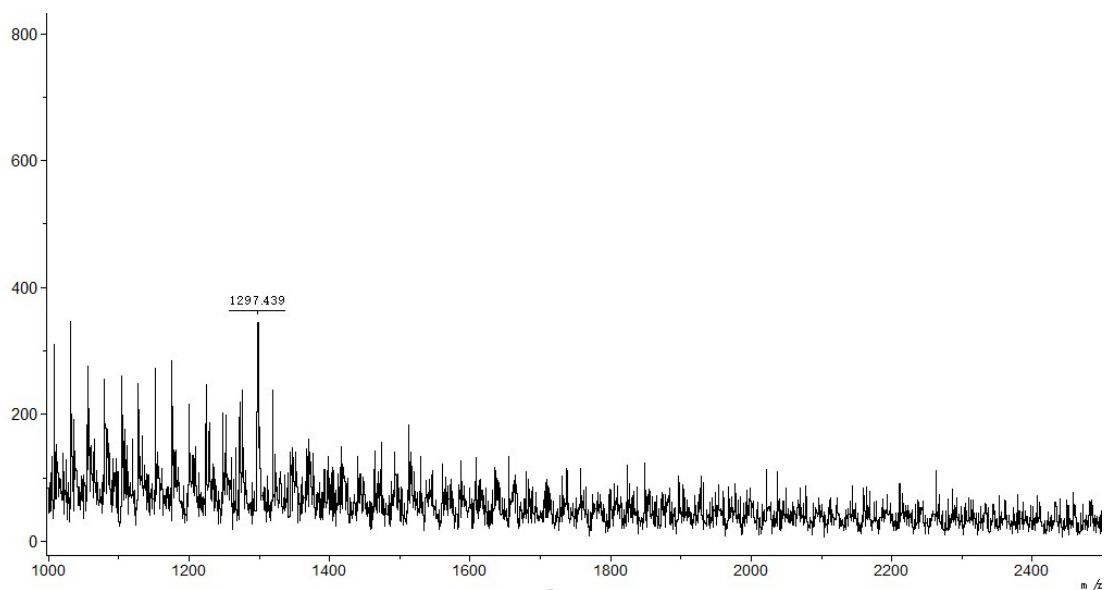


Fig.S9 HRMS spectrum of **DPP2**.

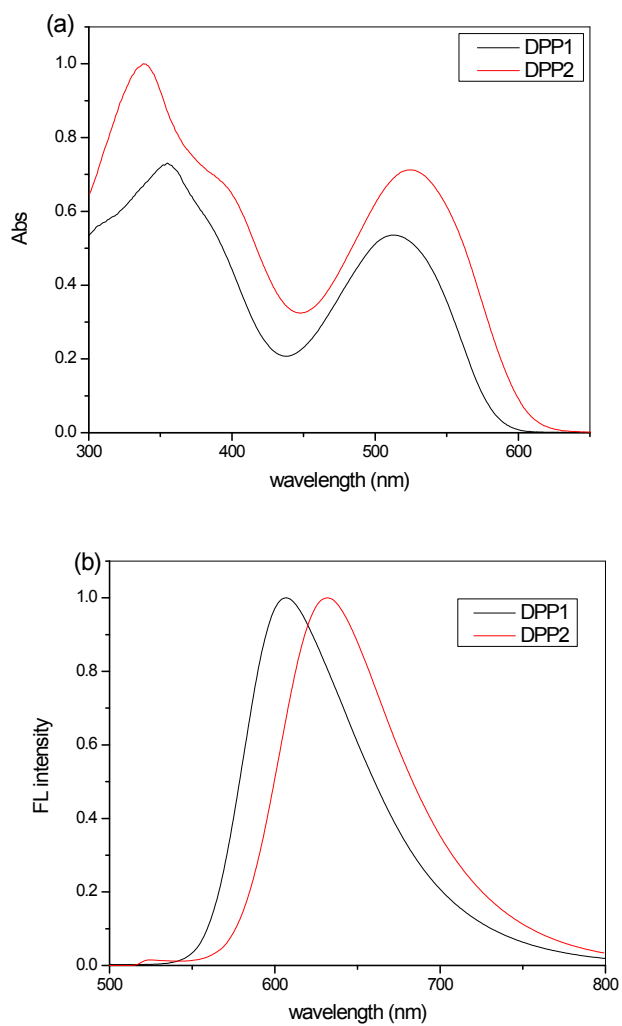


Fig.S10 (a) Normalized UV-vis and (b) photoluminescence (PL) spectra of **DPP1** and

DPP2 in THF.

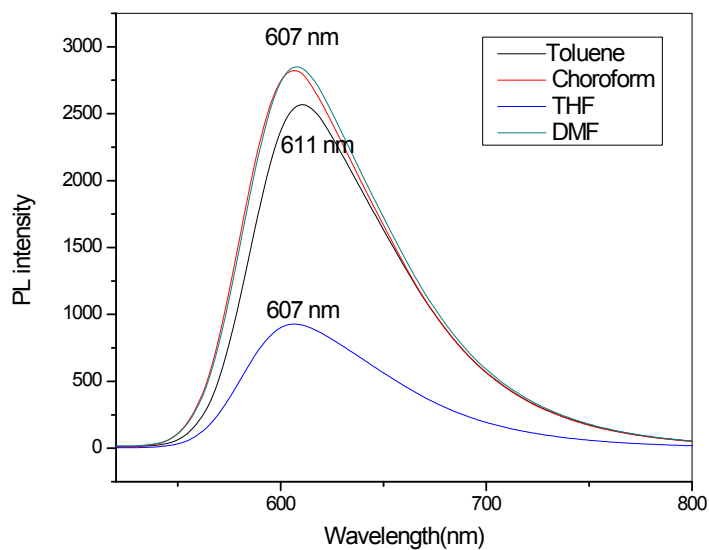


Fig.S11 The photoluminescence (PL) spectra of **DPP1** (10 μ M) in different solvents.

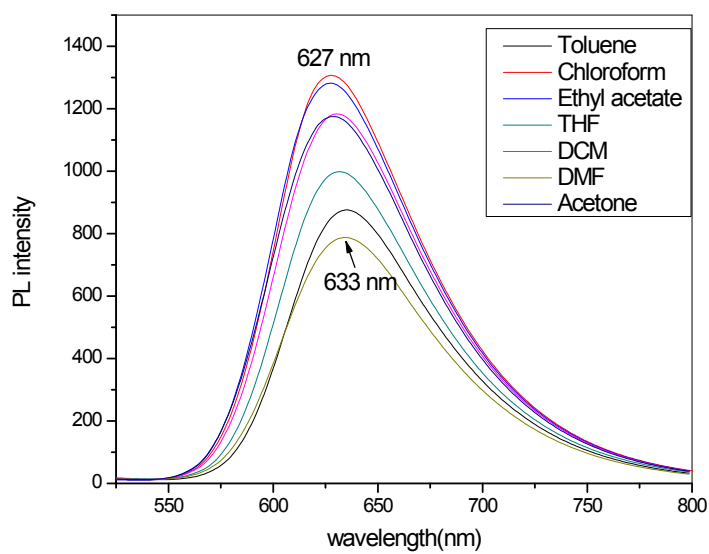


Fig.S12 The photoluminescence (PL) spectra of **DPP2** (10 μ M) in different solvents.

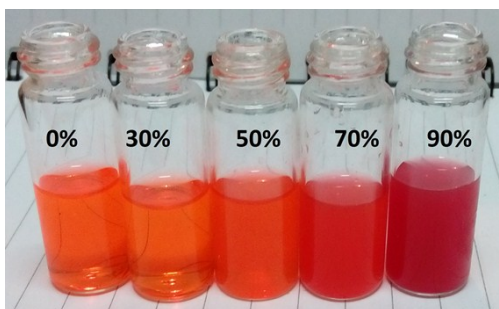
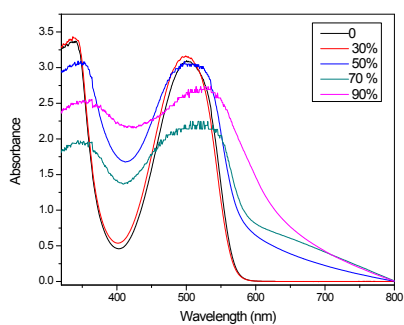


Fig.S13 The UV-vis spectra of **DPP1** (10 μ M) in THF/water.

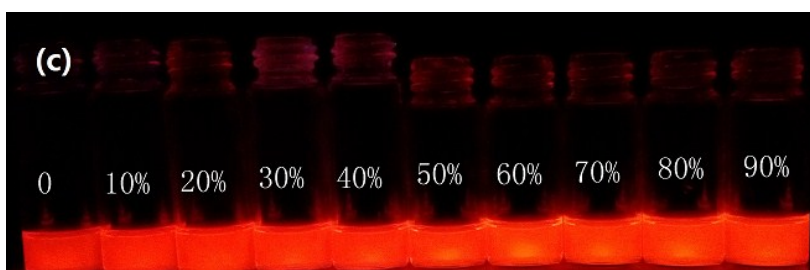
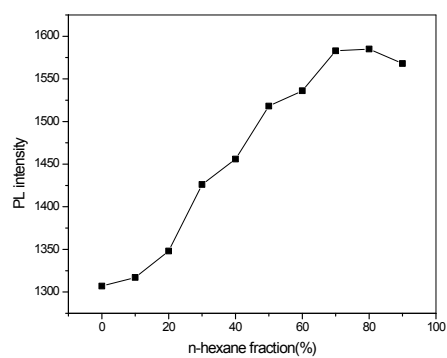
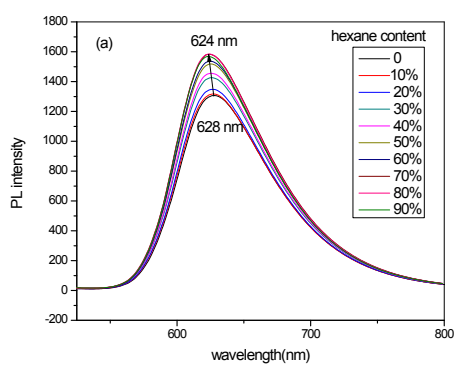


Fig. S14 (a) The photoluminescence (PL) spectra, (b) PL intensity vs f_h and (c) emission photographs of **DPP2** in CHCl_3 /hexane mixtures with different f_h values.

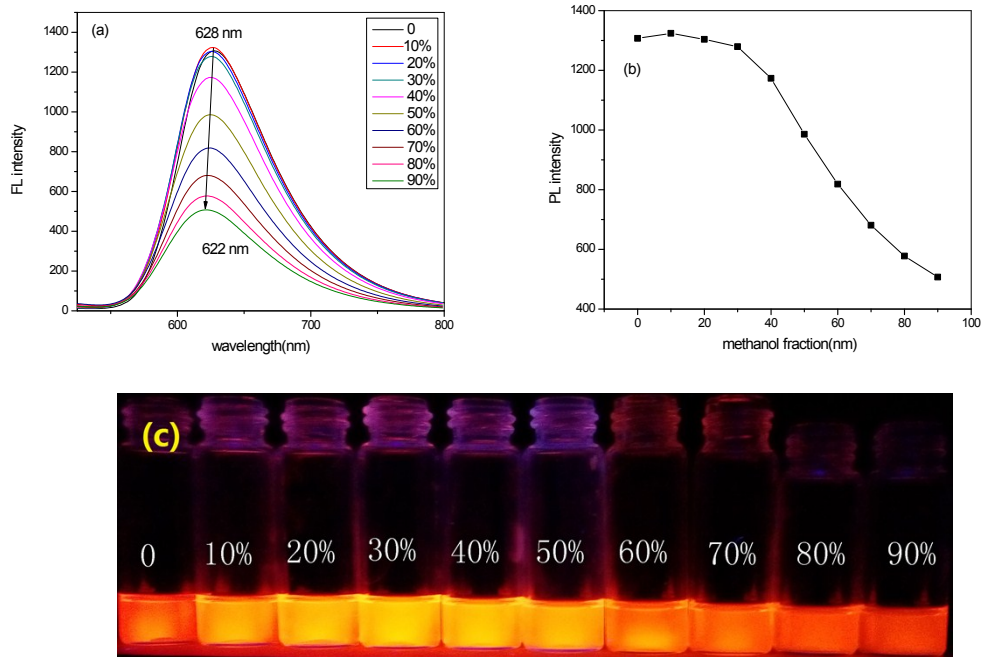


Fig.S15 (a) The photoluminescence (PL) spectra spectra, (b) PL intensity vs f_m and (c) emission photographs of **DPP2** in CHCl₃/methanol mixtures with different f_m values.

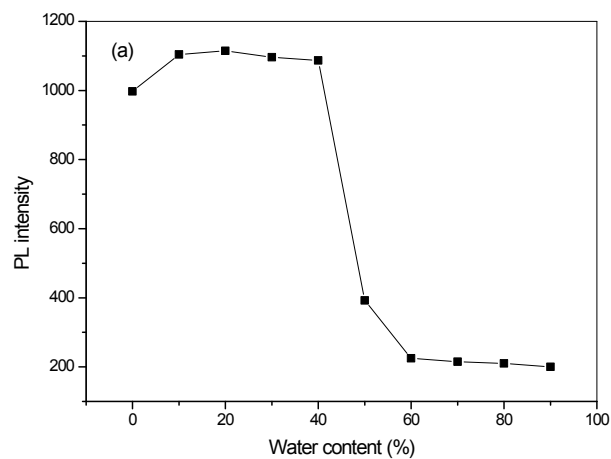


Fig.S16 (a) PL intensity vs f_w and (b) emission photographs of **DPP2** in THF/water mixtures with different f_w values.



Fig. S17 The photographs of compound **4** in daylight (left) and under 365 nm excitation (right).

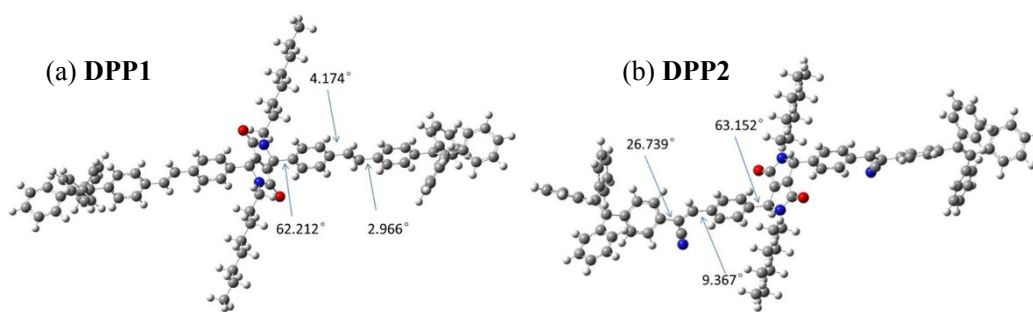


Fig.S18 The optimizations of the molecular geometry by theoretical calculation.

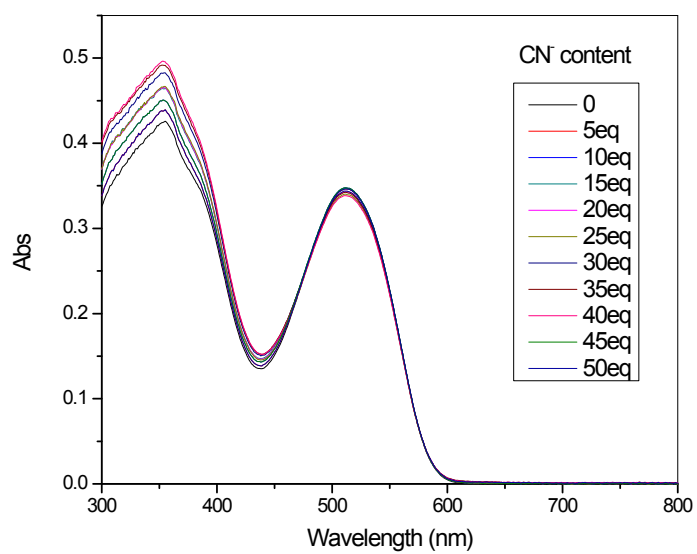


Fig. S19 UV-Vis spectral changes of **DPP1** in THF ($10 \mu\text{M}$) with the increasing concentrations of cyanide anion.

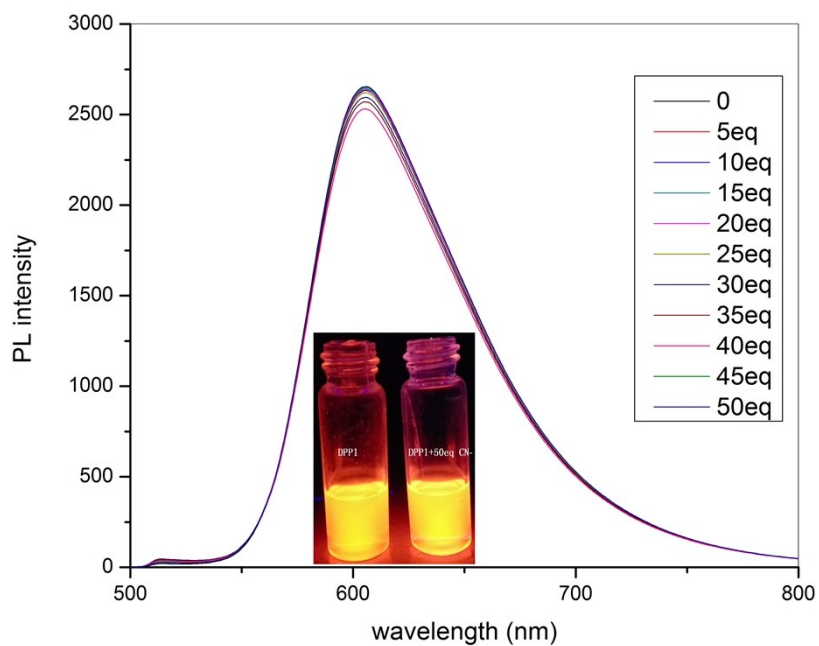


Fig. S20 The photoluminescence (PL) spectral changes of **DPP1** (10 μM) in THF with the increasing concentrations of CN⁻ in THF under excitation at 510 nm.

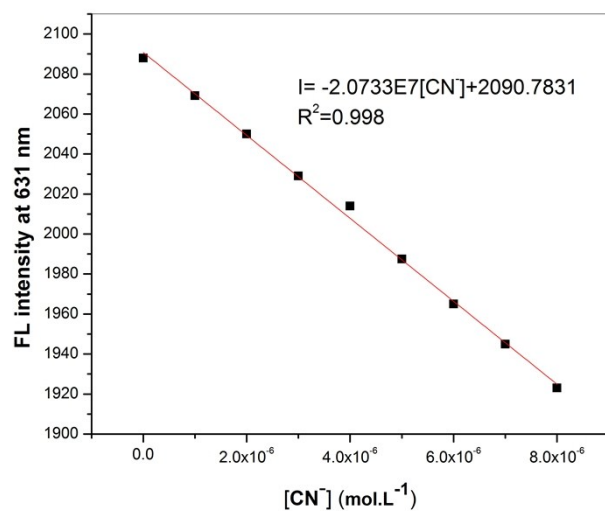


Fig.S21 The linear relation for concentration of CN⁻ in the range of 1–8 μM.

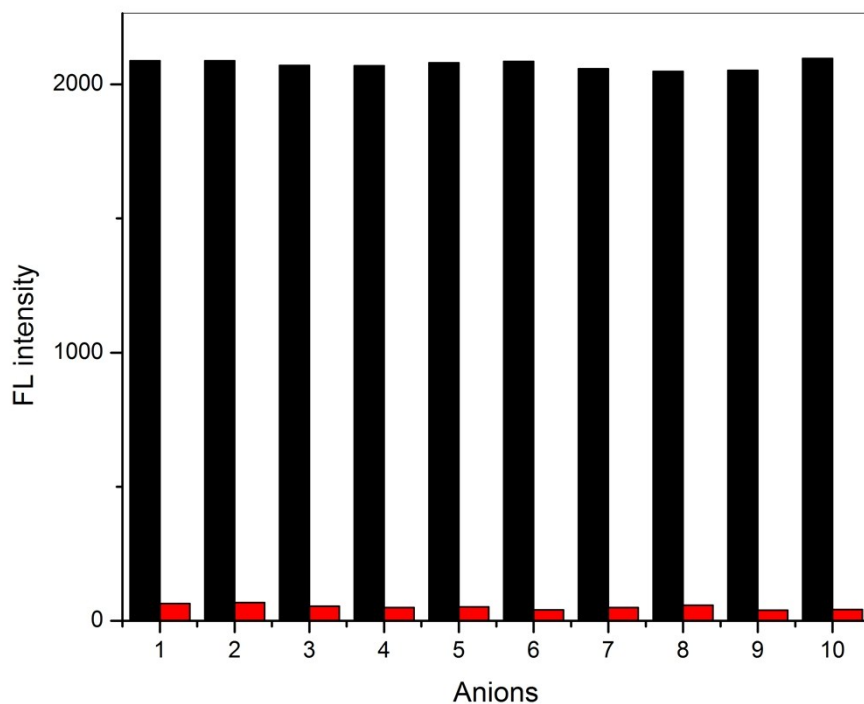


Fig. S22 Selectivity of **DPP2**. The black bars represent fluorescence intensity at 631nm of **DPP2** in THF in the presence of other anions (52 equiv). The red bars represent the fluorescence intensity that occurs upon the subsequent addition of 52 equiv of CN^- to the above solution. From 1 to 10, control, F^- , Cl^- , Br^- , I^- , HSO_4^- , H_2PO_4^- , OAc^- , NO_3^- and ClO_4^- .

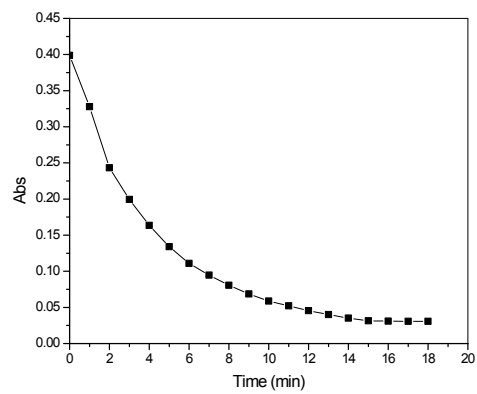


Fig. S23 Time-dependent absorption intensity of probe **DPP2** (10 μM) in THF at 525 nm in the presence of CN^- (24 equiv) at room temperature.